Supplementary Information

Tin Halide Perovskite Solar Cells with Open-Circuit Voltages Approaching the Shockley-Queisser Limit

Wentao Liu,[a] Shuaifeng Hu,[a] Jorge Pascual,[a] Kyohei Nakano,[b] Richard Murdey,[a] Keisuke Tajima,[b] and Atsushi Wakamiya[*,a]*

*E-mail: wakamiya@scl.kyoto-u.ac.jp

Experimental section

Materials

Formamidinium iodide (FAI, 99.99%) and bathocuproine (BCP) were purchased from Tokyo Chemical Industry Co., Ltd. (TCI). Ammonium thiocyanate (NH_4SCN, 99.99% trace metals basis), tin(II) fluoride (SnF_2, 99%), and tin(II) iodide (SnI_2, beads, 99.99%, trace metals basis), ethane-1,2-diammonium iodide (ethylenediammonium diiodide, $EDAI_2$, ≥98%), and poly(methyl methacrylate) (PMMA) were purchased from Sigma-Aldrich Co., Ltd. (Sigma-Aldrich). Poly (3,4-ethylenedioxythiophene): poly (styrene sulfonate) (PEDOT:PSS) aqueous solution (Clevious PVP AI 4083) was purchased from Heraeus Co., Ltd. Fullerene C_{60} (sublimed, 99.99%) was purchased from ATR Company. Indene-C_{60} bisadduct (ICBA) was purchased from Ossila. Dehydrated dimethyl sulfoxide (DMSO, super dehydrated), dehydrated orthodichlorobenzene (*o*-DCB), and dehydrated 1,2,4-trichlorobenzene (TCB) were purchased from FUJIFILM Wako Pure Chemical Co., Ltd. Dimethylformamide (DMF), toluene, and chlorobenzene were purchased from Kanto Chemical. Co., Inc. All of these solvents were degassed by Ar gas bubbling for 1 h and further dried with molecular sieves (3 Å) in an Ar-filled glove box (H_2O, O_2 <0.1 ppm) before use. All the materials were used as received.

Preparation of perovskite films

0.8 mol/L (M) $PEA_{0.15}FA_{0.85}SnI_3$ perovskite solution was prepared by dissolving PEAI (30.0 mg, 0.12 mmol), FAI (116.9 mg, 0.68 mmol), SnI_2 (298.0 mg, 0.8 mmol) SnF_2 (9.4 mg, 0.06 mmol) and NH_4SCN (3.0 mg, 0.04 mmol) in a mixed solvent of 0.8 mL DMF and 0.2 mL DMSO. The precursor solution was stirred at 70 °C for 1 h and filtered through a 0.20 μm PTFE filter before spin-coating. After the precursor solution was cooled down to room temperature, 200 μL of the precursor solution was spin-coated at 5000 rpm for 50 s with an acceleration of 1000 rpm s^{-1} (total time for spin-coating is 55 s). 500 μL of toluene antisolvent was dripped onto the surface of the spinning substrate at 52 s during the spinning. Then, the substrate was immediately annealed on a 70 °C hot plate for 10 min. All the steps above were conducted in an Ar-filled glove box (H_2O, O_2 < 0.1 ppm).

Device fabrication

Glass/ITO substrates (10 Ω sq^{-1}, Geomatec Co., Ltd.) were etched with zinc powder and HCl (6 M in deionized water), then consecutively cleaned with water, acetone, detergent solution (Semico Clean 56, Furuuchi chemical), water, and isopropyl alcohol with 15 min ultrasonic bath under each step. Before coating the PEDOT:PSS, the plasma treatment was applied for cleaning the substrates. PEDOT:PSS aqueous dispersion was filtered through a 0.45 μm PTFE filter and then spin-coated on the ITO glass surface at 500 rpm for 10 s and 4000 rpm for 30 s, and then annealed at 140 °C for 20 min under air. The substrates were transferred to an Ar-filled glove box (H_2O, O_2 < 0.1 ppm) and annealed at 140 °C for another 20 min. The perovskite layer was fabricated on PEDOT:PSS following the above-mentioned procedure. For $EDAI_2$ post-treatment, 1.0 mg $EDAI_2$ was added to 1.0 mL IPA and 1.0 mL toluene. The mixed solution was stirred at 70 °C for 3h and then filtered through a 0.20 μm PTFE filter before spin coating. After that, 150 μL solution was dynamically spin-coated onto perovskite films. The spin coating process was set as 4000 rpm for 20 s with an acceleration of 1333 rpm s^{-1}. Following spin coating, the films were immediately annealed at 70 °C for around 5 min. Subsequently, 20 mg mL^{-1} solution of ICBA in CB, CB/*o*-DCB (1/1, v/v) or CB/ TCB (10/1, v/v) was spin-coated at 2000 rpm for 30 s, followed by annealing at 70 °C or 100 °C for 10 min. 8 nm of bathocuproine (0.01 nm s^{-1}) was then deposited by thermal evaporation. Finally, 100 nm of Ag was deposited through a shadow mask to form the metal electrode. The deposition rate for Ag was set as 0.003 nm s^{-1} until the thickness reached 5 nm, then 0.01 nm s^{-1} until 20 nm, and finally 0.08 nm s^{-1} until the target thickness was reached. The device area was approximately 0.15 cm^2.

Characterization

Scanning electron microscopy (SEM) was performed with a Hitachi S8010 ultra-high-resolution scanning electron microscope (Hitachi High-Tech Corporation).

Atomic force microscopy (AFM) was performed with a Picoscan Plus AFM instrument used in AC-mode with Nanoworld NCST probes.

Ultraviolet photoelectron spectroscopy (UPS) was performed with a photoelectron spectroscopy system (PHI5000 Versa Probe II, ULVAC-PHI Inc.) with He I excitation (21.22 eV). A −5.0 V bias was applied to the samples. The chamber base pressure was approximately 1×10^{-6} Pa. Samples were transferred from the glove box to the UPS chamber without air exposure.

UV–vis absorption measurement was performed with a Shimadzu UV-3600 plus spectrometer (Shimadzu Co., Ltd.).

XRD measurements were performed on a Rigaku RINT 2500 (Rigaku Co.) diffractometer. Perovskite films were deposited on the surface of PEDOT:PSS with glass/ITO as substrates and covered with a thin film of spin coated poly(methyl methacrylate) (PMMA, Sigma–Aldrich Co.) to prevent direct exposure to air.

The contact angle measurements of the ICBA layers fabricated onto perovskite layers were recorded in a range of 0–180° with high precision (± 0.1° accuracy) using a FAMAS interface measurement and analysis system (Kyowa Interface Science Co., Ltd.).

Photocurrent–voltage (*J*–*V*) curves were measured in a N_2-filled glove box (H_2O, O_2 <0.1 ppm) with an OTENTO-SUN-P1G solar simulator (Bunkoukeiki Co., Ltd.). The light intensity of the illumination source was calibrated using a standard silicon photodiode. Each device was measured with a 10-mV voltage step and a 100 ms time step (i.e., scan rate of 0.1 V s^{-1}) using a Keithley 2400 source meter. The device active area was defined by an optical mask with an area of 0.0985 cm^2.

External quantum efficiency (EQE) were measured with a Bunkoukeiki SMO-250III system equipped with a Bunkoukeiki SM-250 diffuse reflection unit (Bunkoukeiki Co., Ltd.). The incident light intensity was calibrated with a standard SiPD S1337-1010BQ silicon photodiode.

SCLC measurements were measured in the dark with a Keithley 2450 source meter. The voltage was increased logarithmically scanning from low to high voltage.

KPFM measurement was conducted at room temperature using a Bruker NanoScopeV operating in a Bruker Dimension Icon Glovebox under an argon atmosphere (H_2O < 0.1 ppm, O_2 < 0.1 ppm). The AC bias voltage was 4 V and PtIr-coated silicon cantilevers were used.

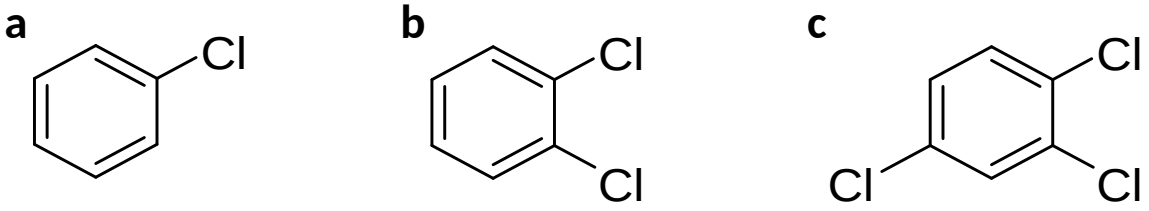

Figure S1. The chemical structures of (a) chlorobenzene (CB), (b) 1,2-dichlorobenzene (o-DCB), and (c) 1,2,4-trichlorobenzene (TCB).

Table S1. The properties of the CB, *o*-DCB, and TCB solvents.

Solvent	CB	o-DCB	TCB
Formula	C_6H_5Cl	$C_6H_4Cl_2$	$C_6H_3Cl_3$
Boiling point (°C)	132.7	180.5	213.5
Vapor pressure (kPa)	1.20	0.16	0.13
Dipole moment (D)	1.50	2.27	1.26

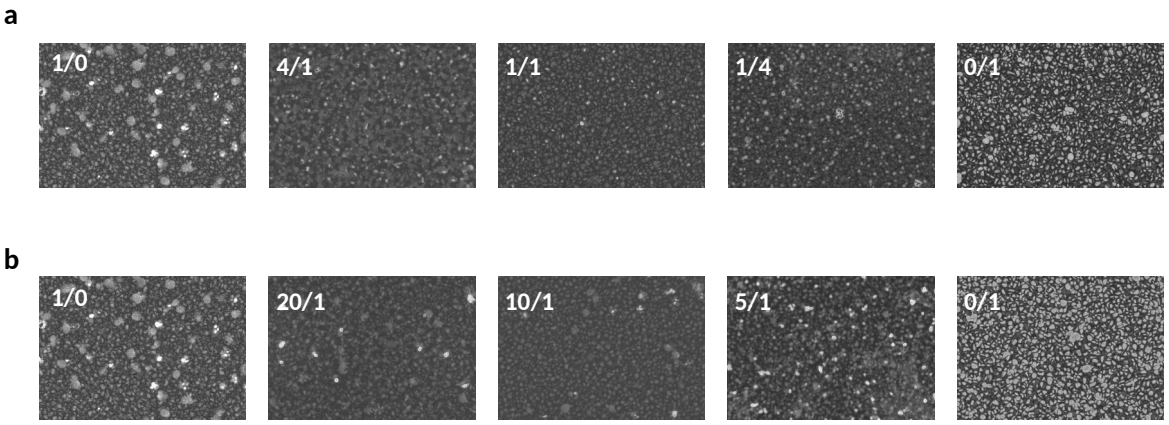

Figure S2. SEM images of ICBA films processed with (a) CB/*o*-DCB and (b) CB/TCB mixed solvent in different volume ratios (scale bars are 2 μm).

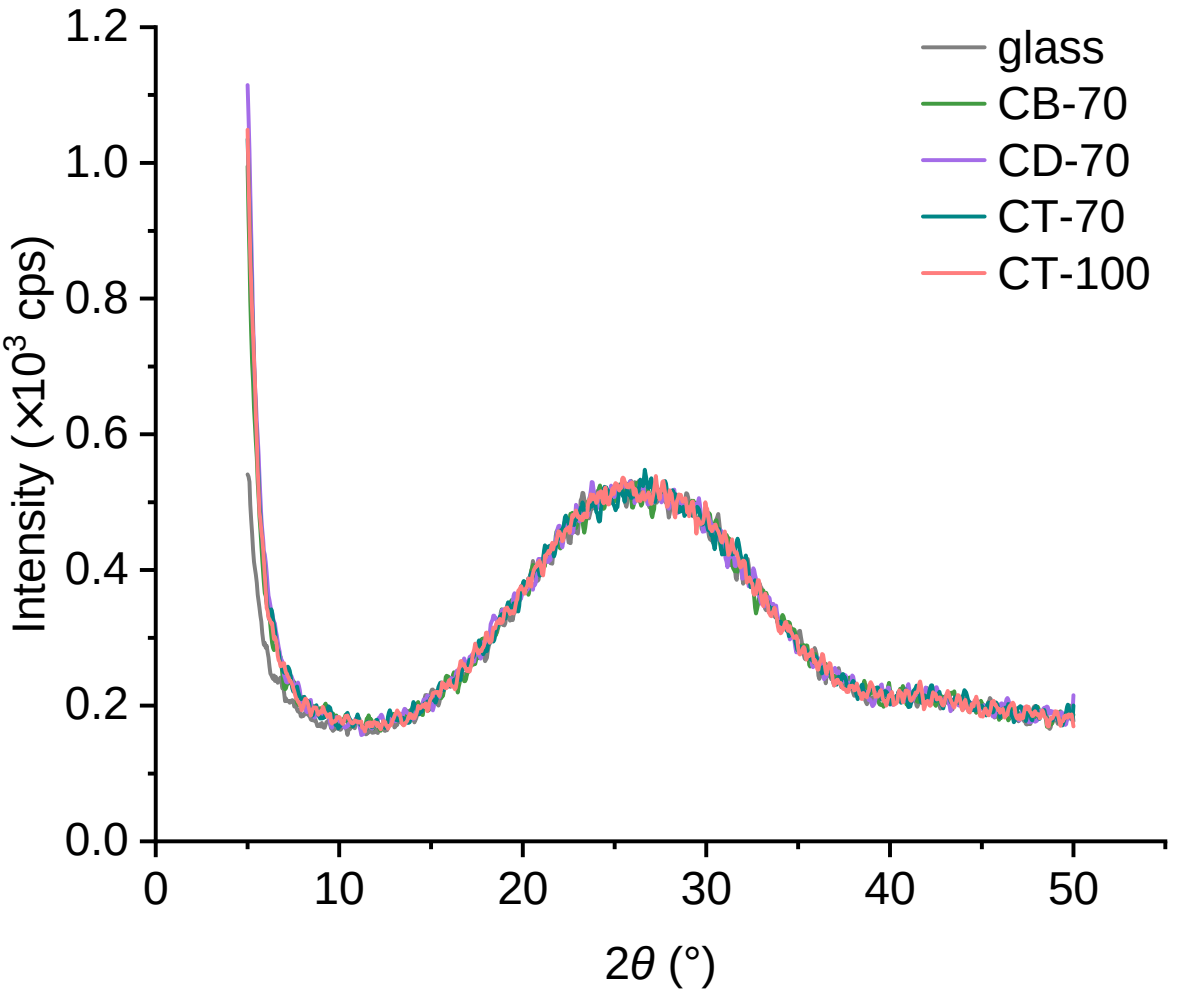

Figure S3. XRD patterns of ICBA films fabricated from **CB-70**, **CD-70**, **CT-70**, and **CT-100** processes on glass substrates.

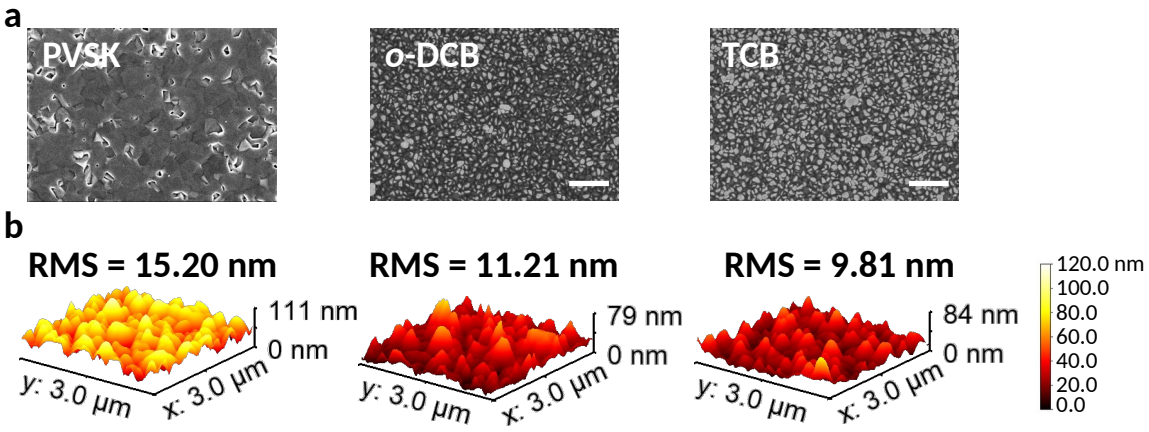

Figure S4. (a) SEM (scale bars are 2 µm) and (b) AFM images of the bare perovskite layer (PVSK) and ICBA-covered perovskite samples prepared from *o*-DCB and TCB solvents.

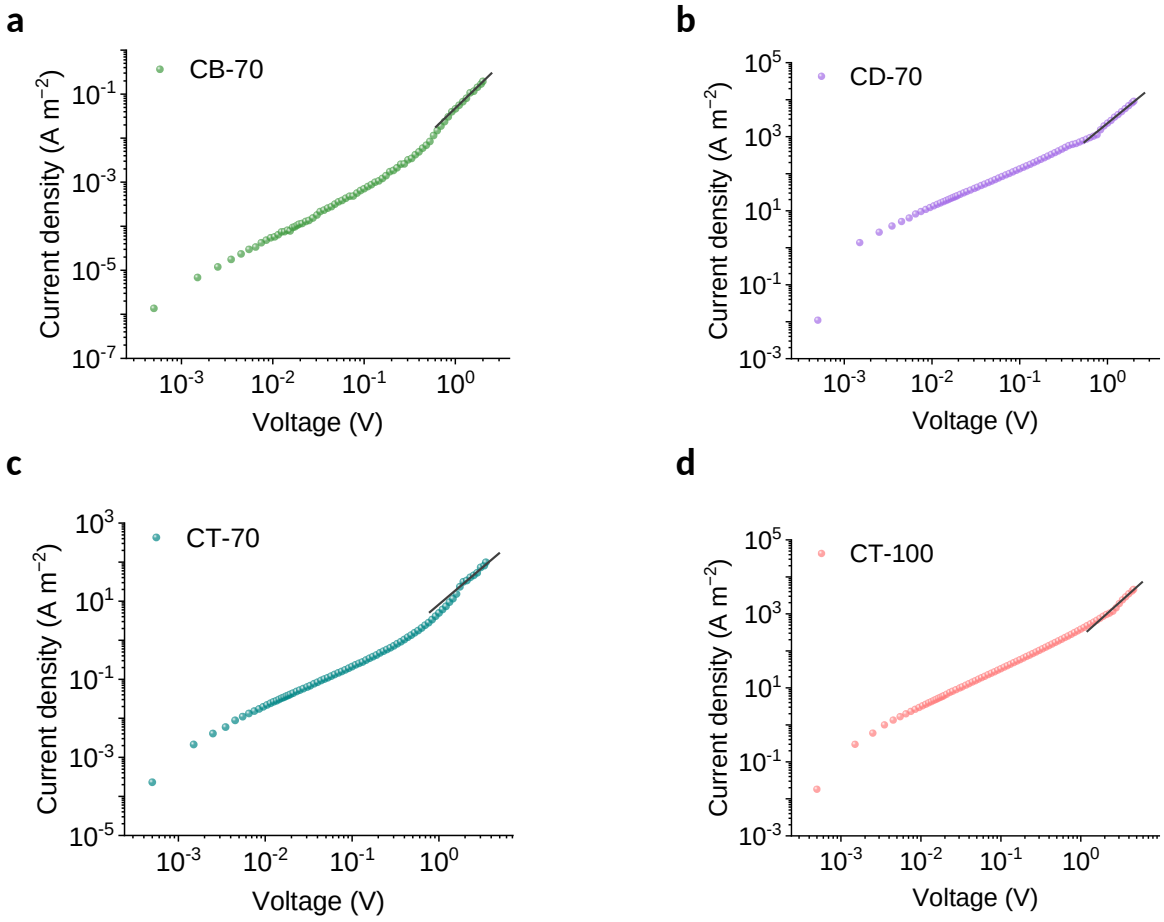

Figure S5. Dark *J*–*V* curves for the electron-only devices with ICBA films fabricated with (a) **CB-70**, (b) **CD-70**, (c) **CT-70**, and (d) **CT-100** processes. Measurements were made at 273K.

Energy level alignment

The energy levels of perovskite and ICBA films were estimated by ultraviolet photoelectron spectroscopy (UPS) and optical absorption measurements. For the perovskite films, a second annealing process at either 70 or 100 °C was applied to examine the influence of annealing temperature on the energy levels. The work function (WF) of perovskite films is estimated as 21.22 eV – $E_{b,\ max}$ with $E_{b,\ max}$ given by the secondary electron cutoff (**Figure S6a**). The valence band maximum (VBM) is estimated as –WF – $E_{b,\ min}$ with $E_{b,\ min}$ obtained from the valence band (VB) region (**Figure S6b**). Combined with the bandgap (E_{bg}) determined from Tauc plot of absorption spectra (**Figure S6c**), the conduction band minimum (CBM) is calculated as VBM + E_{bg}.

The energy level diagram of perovskite annealed at 70 and 100 °C is shown in **Figure S7**. Compared with the films annealed at 70 °C, the bandgap of perovskite films annealed at 100 °C shows an identical value of 1.40 eV, while both CBM and VBM are downshifted by 0.06 eV, from –3.66 to –3.72 eV and from –5.06 to –5.12 eV, respectively. Compared with the films fabricated at 70 °C, the one fabricated under 100 °C presents an increased p-type characteristic, as indicated by the deeper Fermi level. For the ICBA films (**Figures S8–S9**), the calculated lowest unoccupied molecular orbital (LUMO) levels with respect to the vacuum level (E_{vac}) of ICBA films fabricated with **CB-70**, **CD-70**, **CT-70**, and **CT-100** processes are –3.97, –3.89, –3.92, and –3.96 eV, respectively. Accordingly, we summarized the energy level diagram in **Figure S10**. The energy level offsets between the LUMO levels of ICBA films and the CBM of the perovskite layers vary over a range of just 0.08 eV, from 0.23 eV to 0.31 eV. In addition, an almost identical offset was observed for the perovskite and CT-processed ICBA films fabricated under 70 and 100 °C. This suggests that the improved V_{OC} of the solar cells would primarily originate from the substantially reduced energy disorder of the ICBA films while not from the almost identical energy level alignment.

We also measured the work function of the ICBA surface using Kelvin probe force microscope (KPFM). For the KPFM experiments, shown in **Figures S11-S12**, the contact potential difference (CPD) between the tip and the sample is measured by applying an alternating voltage, and the CPD corresponds to the difference between the work function of the sample and the probe. The average CPD varied from 0.394 V for the **CD-70** processed film to 0.500 V for the **CB-70** processed film. Compared with the **CB-70** and **CT-100** processed ICBA films, the surface potentials of the **CD-70** and **CT-70** processed films have notably more narrow distributions. There is no clear relationship

between the variation in the surface potential of ICBA films processed under different conditions and the V_{OC} in the resultant devices. Unfortunately, the broadened density of state (DOS) in the band edge that is responsible for the increased energy disorder of the ICBA films cannot be detected with KPFM.

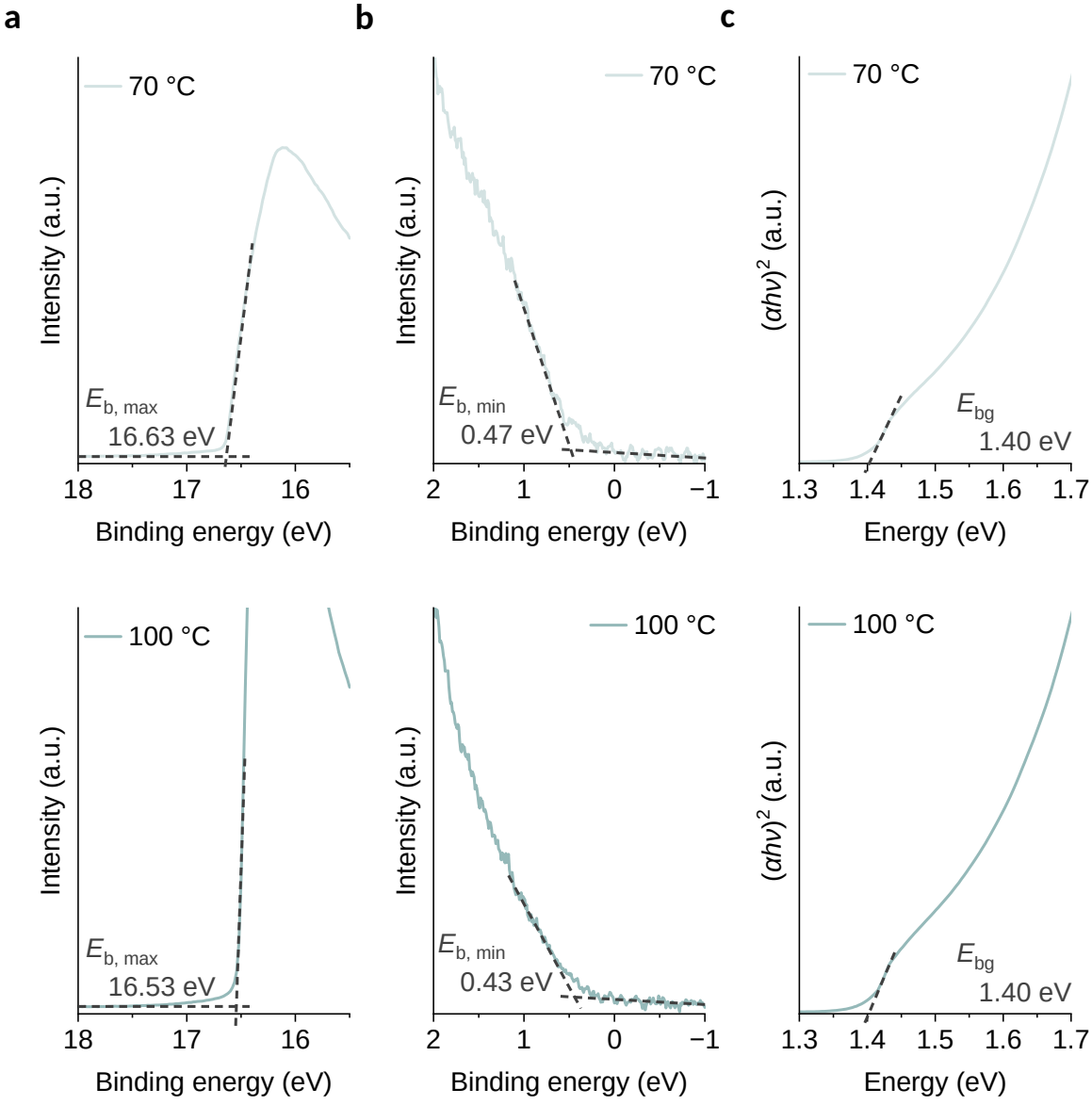

Figure S6. (a) Secondary electron cut-off and (b) valence band (VB) regions of the UPS spectra and (c) Tauc plots of absorption spectra for the $PEA_{0.15}FA_{0.85}SnI_3$ perovskite films annealed under 70 and 100 °C at the second step. The work function (WF) is 21.22 eV – $E_{b, max}$, with $E_{b, max}$ being determined from the secondary electron cut-off. The valence band maximum (VBM) is – 21.22 eV + ($E_{b, max}$ – $E_{b, min}$). The bandgap (E_{bg}) is estimated from Tauc plots of UV-vis absorption spectra. The conduction band minimum (CBM) is VBM + E_{bg}.

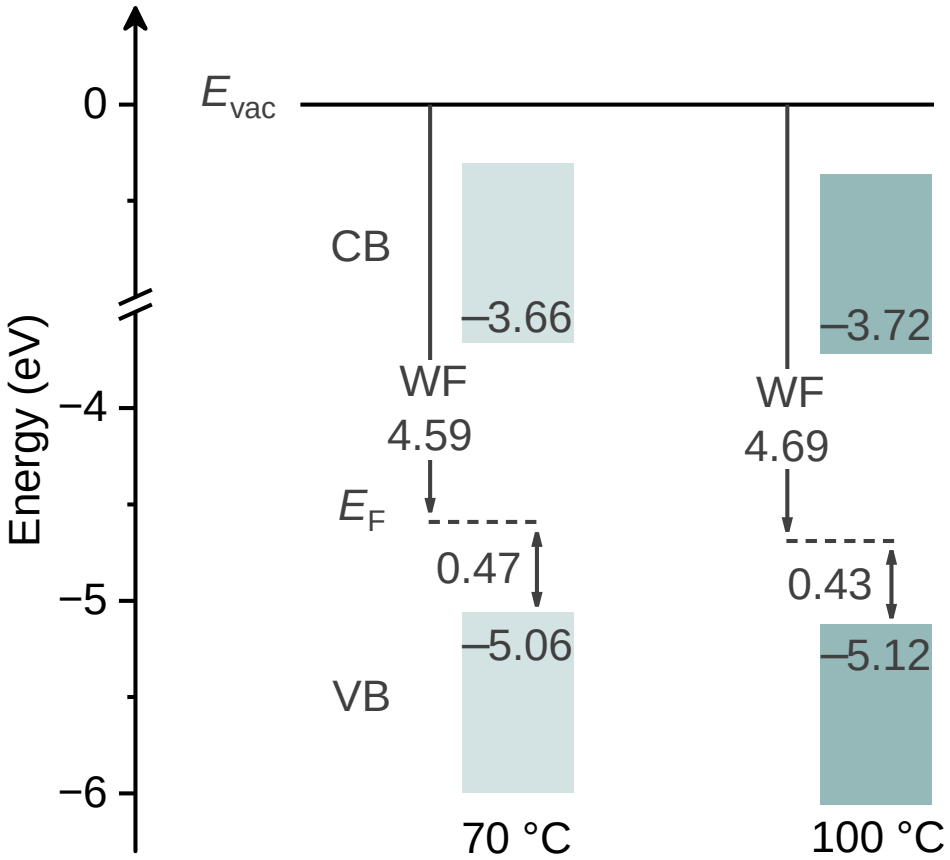

Figure S7. Energy level diagram of $PEA_{0.15}FA_{0.85}SnI_3$ perovskite films with a second annealing step at 70 and 100 °C. Energies are given in electron volts (eV) relative to E_{vac} (vacuum level). E_F (Fermi level) is −WF (work function). CB and VB are the conduction band and valence band of the perovskite layers, respectively. The detailed UPS and absorption spectra are given in **Figure S6**.

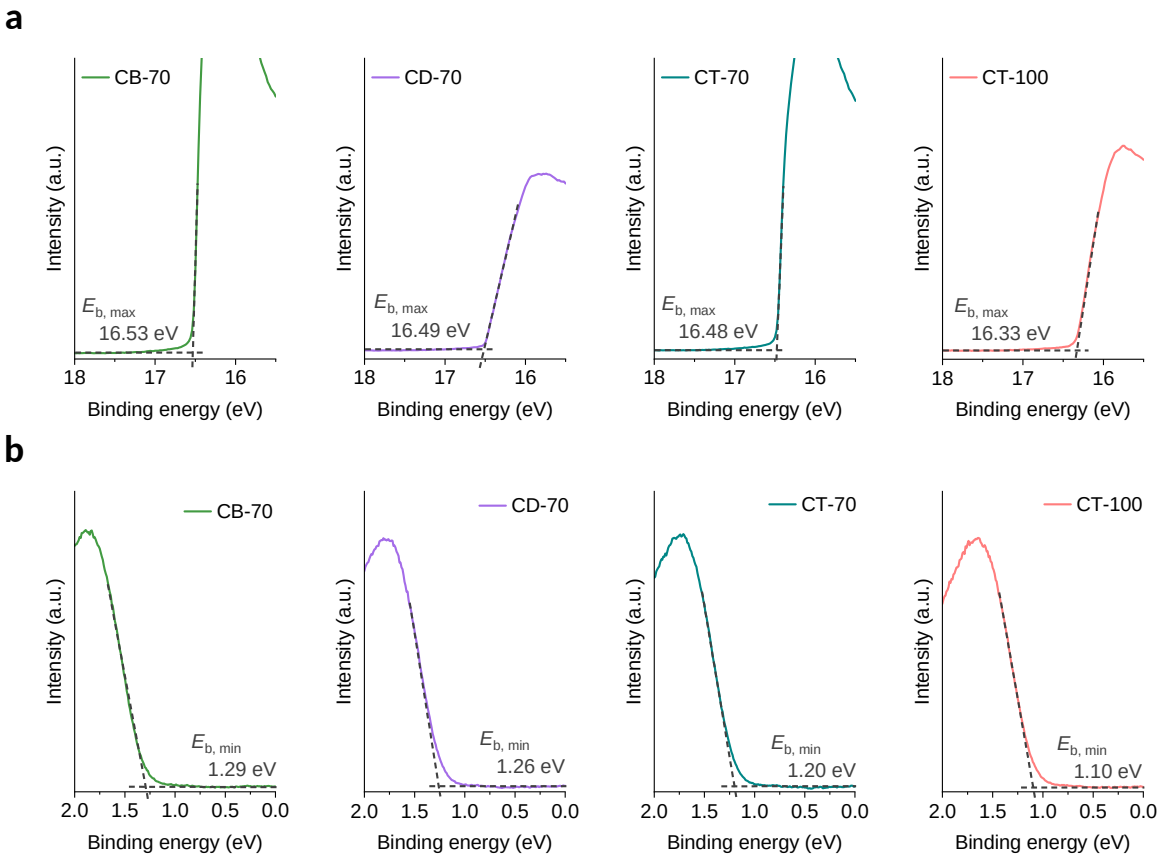

Figure S8. (a) Secondary electron cut-off and (b) valence band (VB) regions of the UPS spectra for the ICBA films fabricated with **CB-70**, **CD-70**, **CT-70**, and **CT-100** processes. The work function (WF) is 21.22 eV – $E_{b, max}$, with $E_{b, max}$ determined from the secondary electron cut-off. The valence band maximum (VBM) is 21.22 eV – ($E_{b, max}$ – $E_{b, min}$).

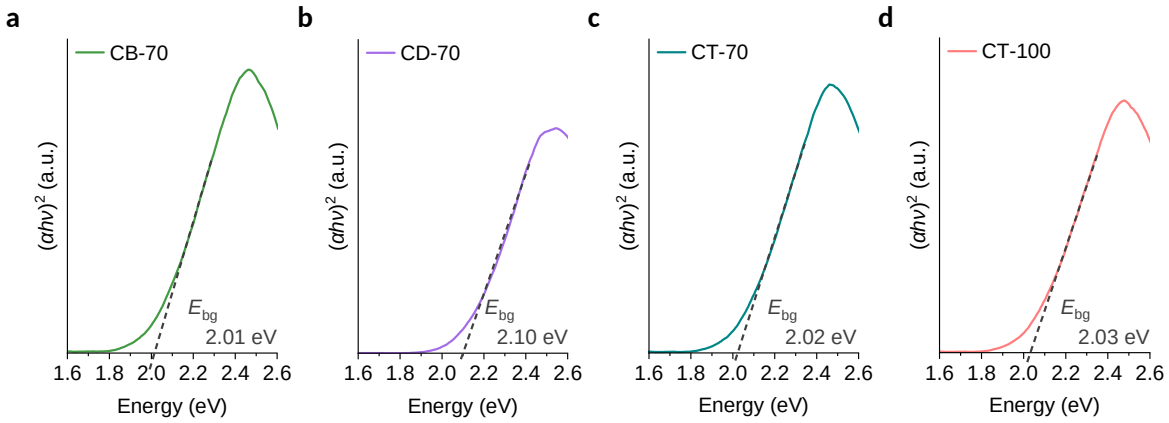

Figure S9. Tauc plots of the absorption spectra for ICBA films fabricated with (a) **CB-70**, (b) **CD-70**, (c) **CT-70**, and (d) **CT-100** processes. The bandgap (E_{bg}) of ICBA films is estimated through the x-intercept of the tangent line.

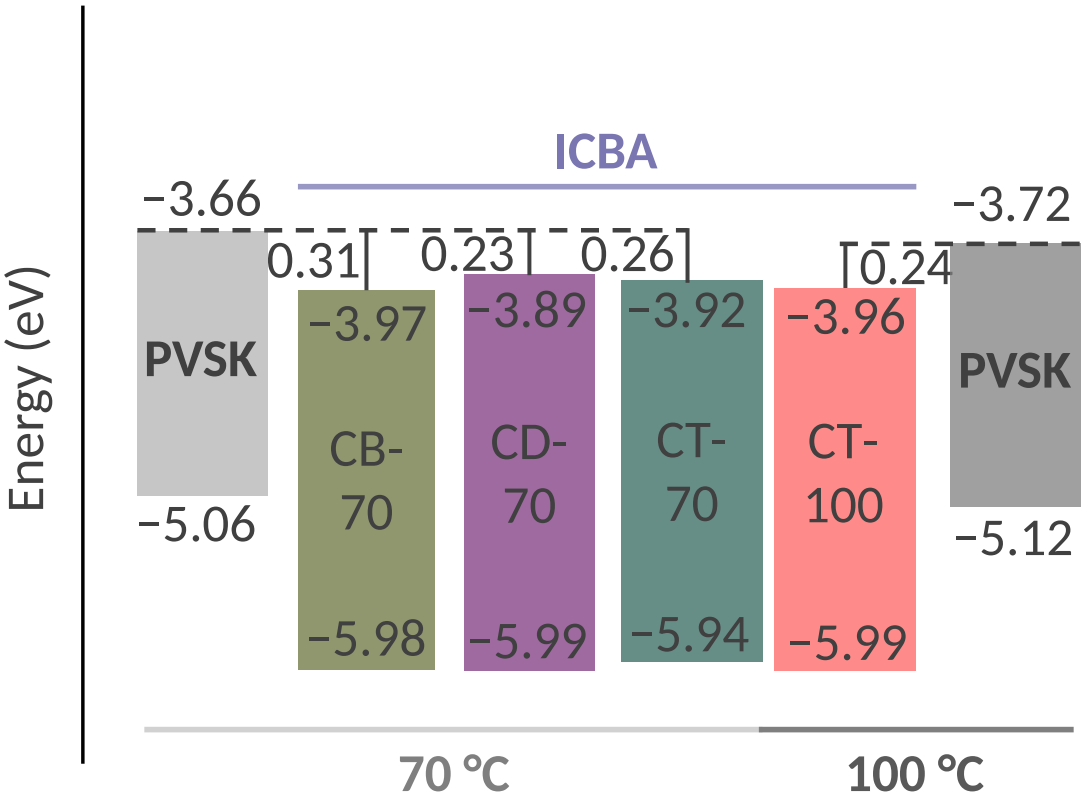

Figure S10. Energy level diagram for the $PEA_{0.15}FA_{0.85}SnI_3$ perovskite films (PVSK) after a second annealing step at either 70 or 100 °C, and ICBA films processed from **CB-70**, **CD-70**, **CT-70**, and **CT-100**.

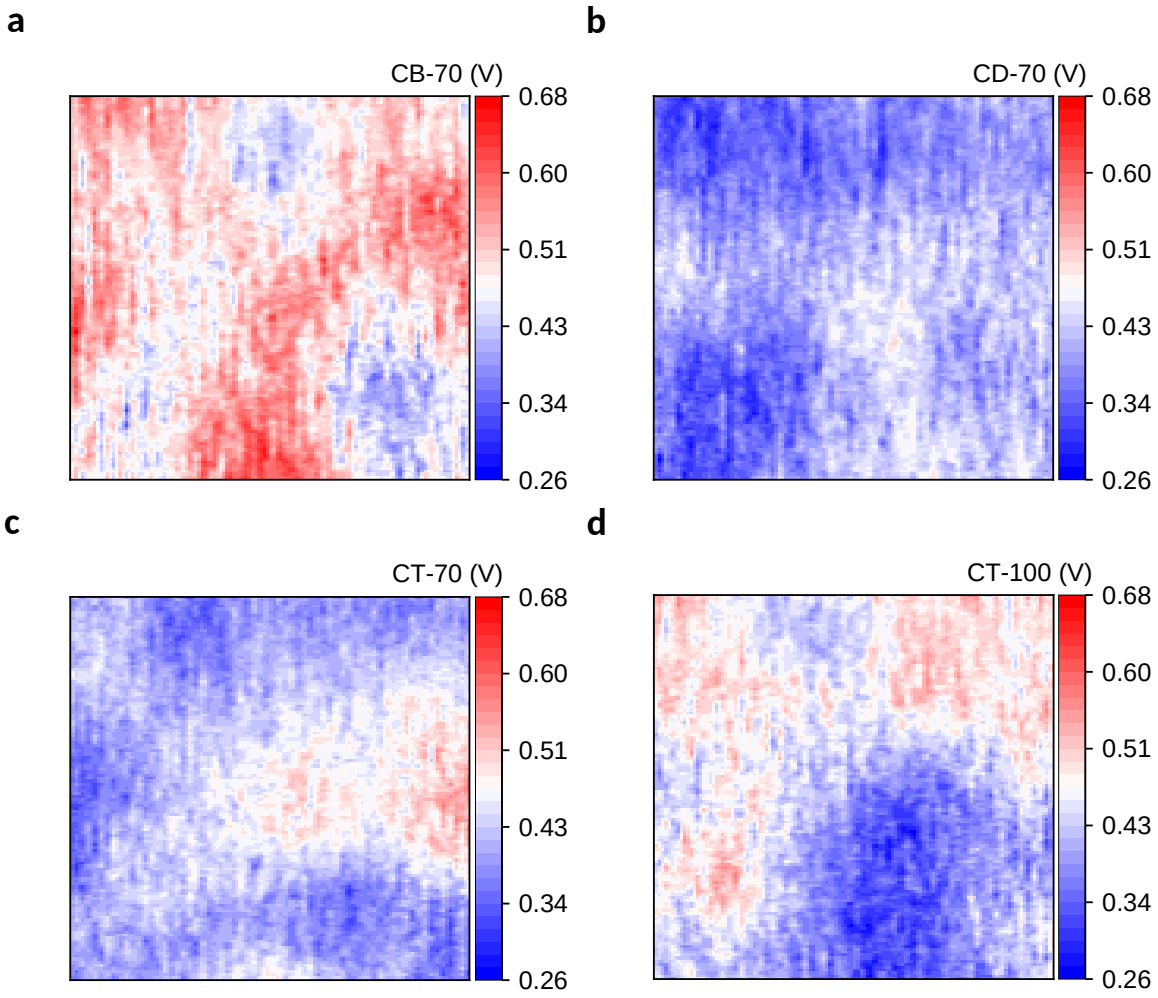

Figure S11. KPFM mapping in 1 × 1 μm matrix for the ICBA films fabricated from **CB-70** (a), **CD-70** (b), **CT-70** (c), and **CT-100** (d) processes.

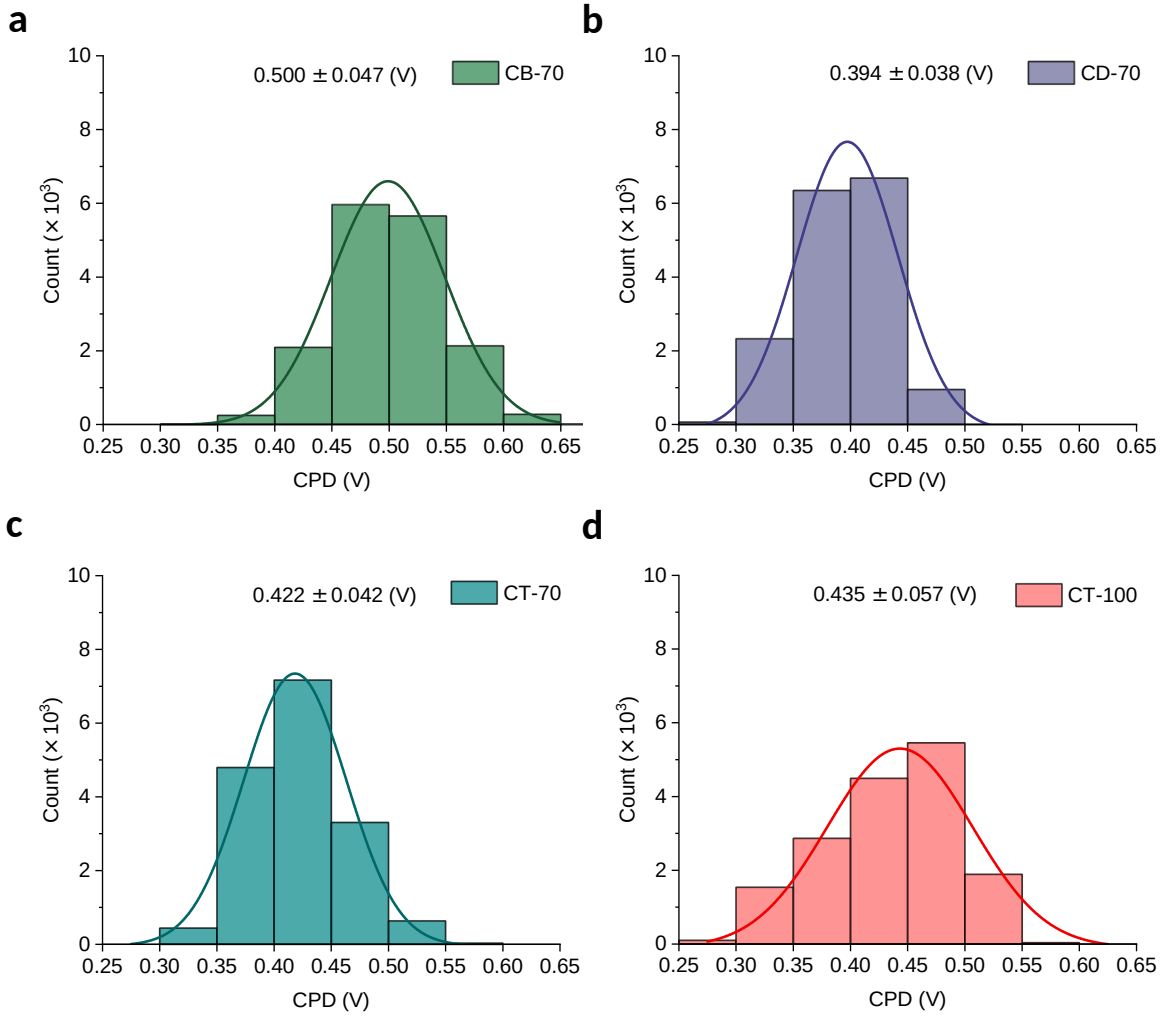

Figure S12. Surface potential difference distribution of ICBA films fabricated from **CB-70** (a), **CD-70** (b), **CT-70** (c), and **CT-100** (d) processes.

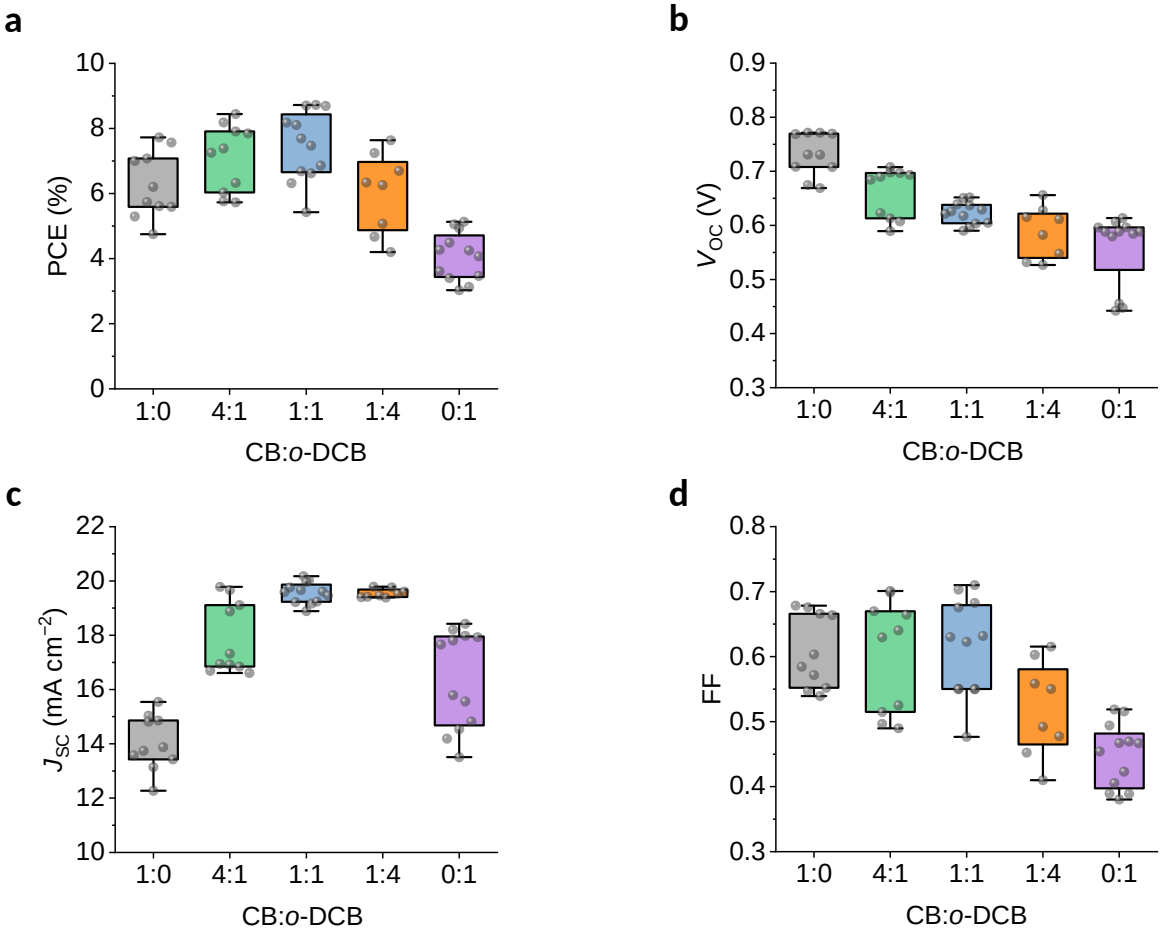

Figure S13. Statistical distribution of (a) PCE, (b) V_{OC}, (c) J_{SC}, and (d) FF for solar cells with ICBA films processed from different volume ratios of CB/*o*-DCB mixed solvent.

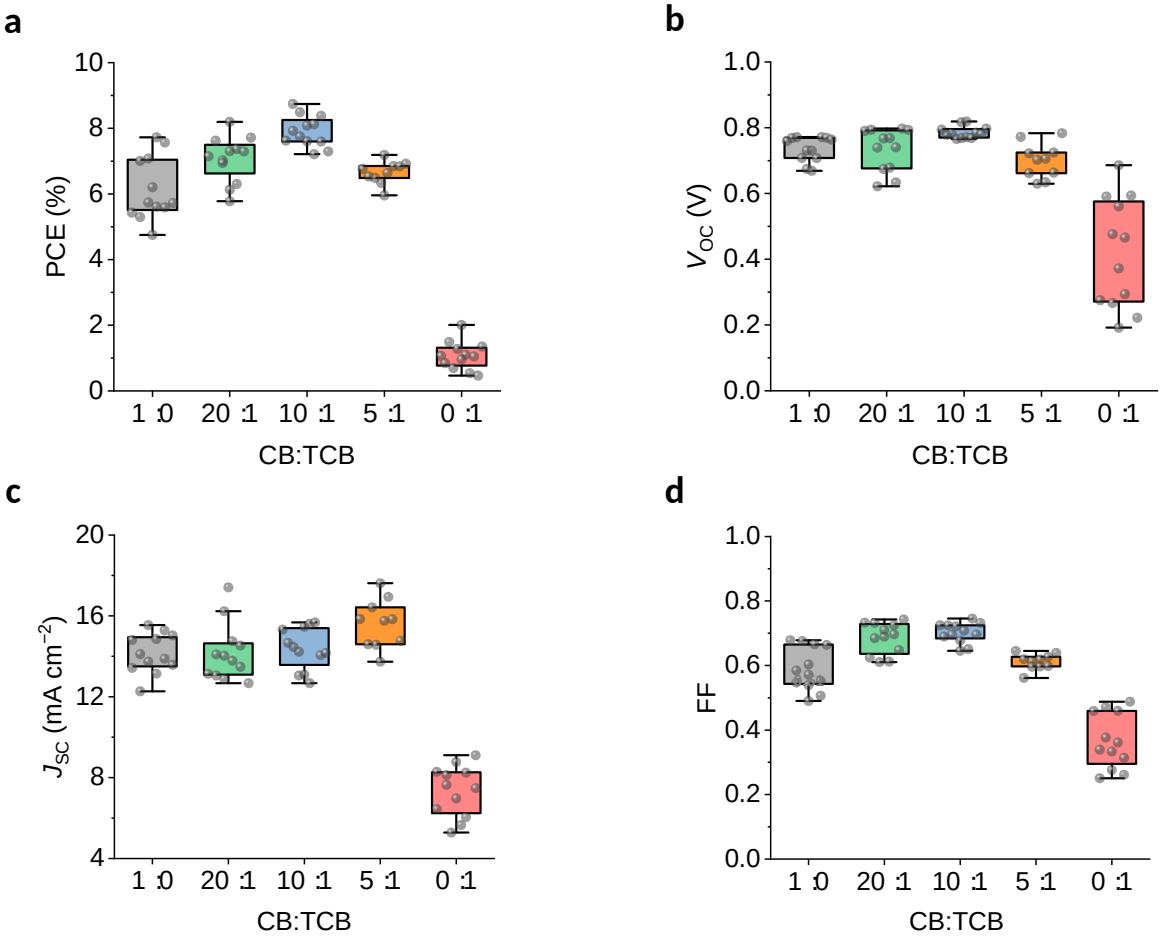

Figure S14. Statistical distribution of (a) PCE, (b) V_{OC}, (c) J_{SC}, and (d) FF for solar cells with ICBA films processed from different volume ratios of CB/TCB mixed solvent.

Table S2. Champion and average PV parameters of PSCs from a single batch of six solar cells.

Conditions	J_{SC} (mA cm^{-2})[a]	V_{OC} (V)[a]	FF[a]	PCE (%)[a]
CB-70	15.04 (14.14 ± 0.94)	0.77 (0.73 ± 0.04)	0.67 (0.59 ± 0.06)	7.73 (6.15 ± 0.92)
CD-70	19.22 (19.56 ± 0.37)	0.64 (0.62 ± 0.02)	0.71 (0.61 ± 0.07)	8.72 (7.46 ± 1.03)
CT-70	15.32 (14.37 ± 0.99)	0.82 (0.79 ± 0.02)	0.70 (0.70 ± 0.03)	8.74 (7.90 ± 0.46)
CT-100	8.70 (7.45 ± 1.01)	0.98 (0.94 ± 0.05)	0.67 (0.60 ± 0.05)	5.70 (4.19 ± 0.75)

[a]The average and standard deviation values are given in parentheses.

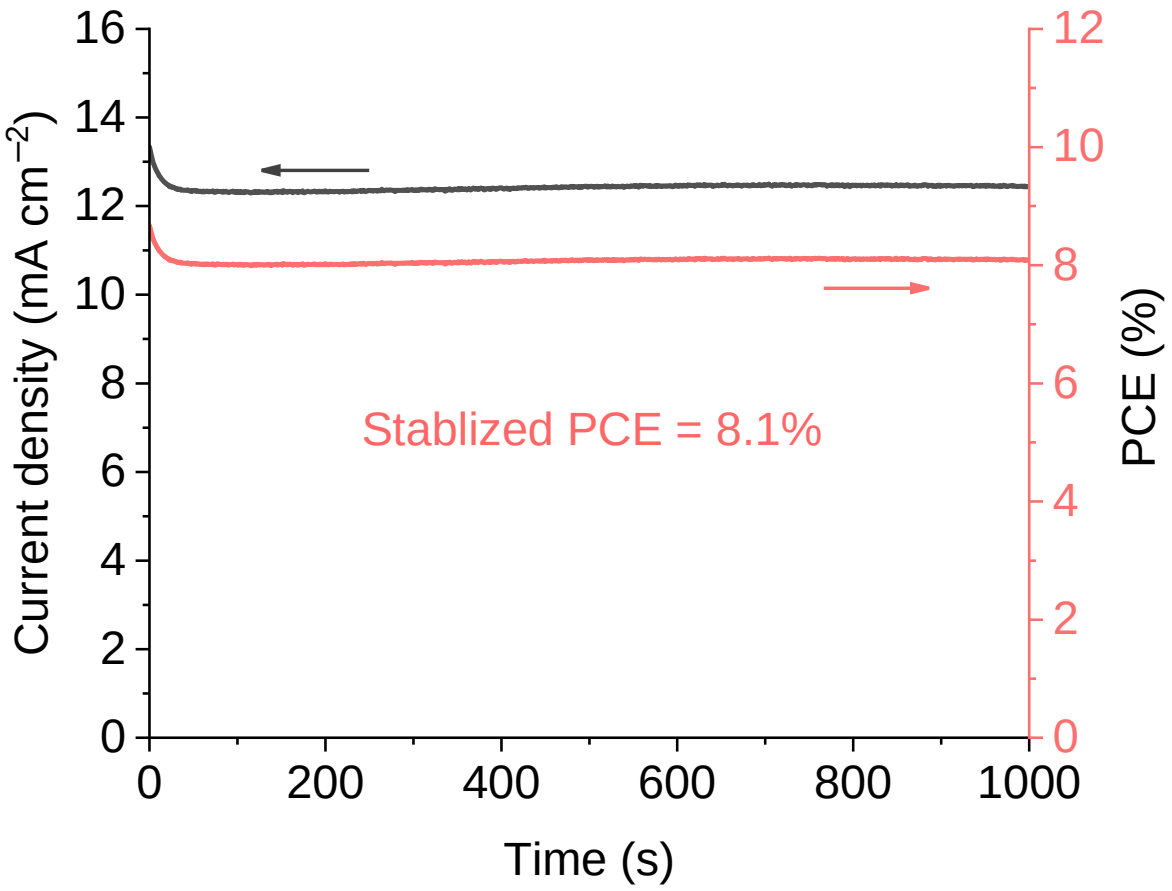

Figure S15. Stabilized power output of the device made with CT-processed ICBA films measured by fixing the voltage at 0.65 V under AM1.5G.

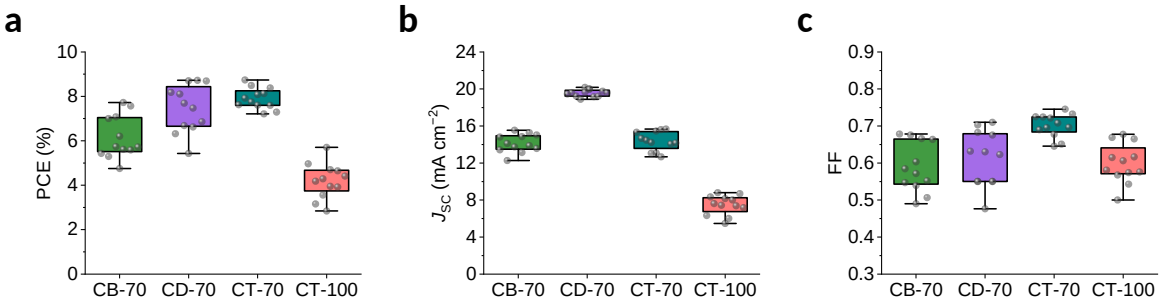

Figure S16. Distributions of (a) PCE, (b) J_{SC}, and (c) FF values derived for six devices from each of the **CB-70**, **CD-70**, **CT-70**, and **CT-100** processes. The data includes values derived from both forward and reverse *J*–*V* scans.

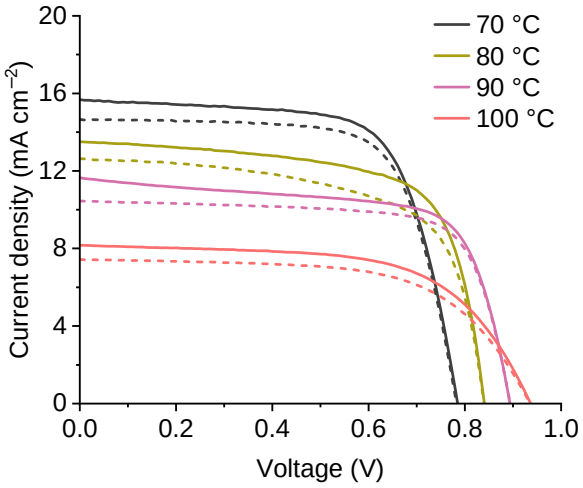

Sample	J_{SC} (mA cm^{-2})	V_{OC} (V)	FF	PCE (%)
70 ◗C-F	15.68	0.78	0.69	8.49
70 ◗C-R	14.66	0.78	0.71	8.13
80 ◗C-F	13.51	0.84	0.68	7.70
80 ◗C-R	12.63	0.84	0.64	6.79
90 ◗C-F	11.65	0.89	0.69	7.18
90 ◗C-R	10.45	0.89	0.73	6.85
100 ◗C-F	8.17	0.94	0.61	4.70
100 ◗C-R	7.44	0.94	0.62	4.29

Figure S17. *J*–*V* curves and performance parameters of the devices fabricated with ICBA films processed with CT mixed solvent under different annealing temperatures.

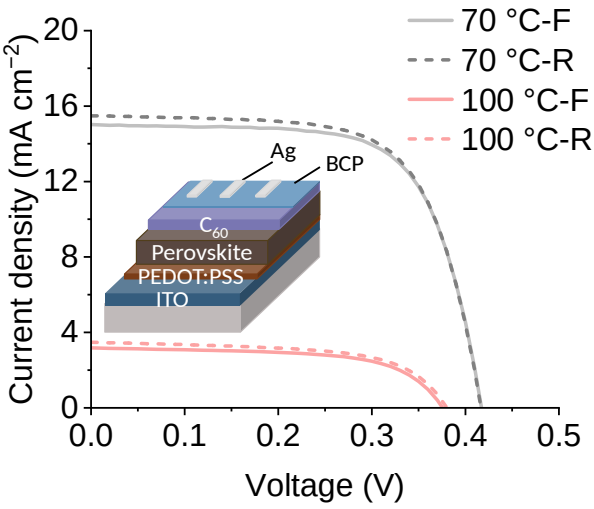

Sample	J_{SC} (mA cm^{-2})	V_{OC} (V)	FF	PCE (%)
70 °C-F	15.02	0.42	0.68	4.28
70 °C-R	15.48	0.42	0.67	4.35
100 °C-F	3.18	0.38	0.62	0.74
100 °C-R	3.48	0.38	0.61	0.80

Figure S18. *J–V* curves and performance parameters of the devices with C_{60} as ETL. The annealing process of perovskite films is 70 °C for 10 min, and then 70 °C and 100 °C for another 10 min for the cells denoted as 70 °C and 100 °C, respectively.

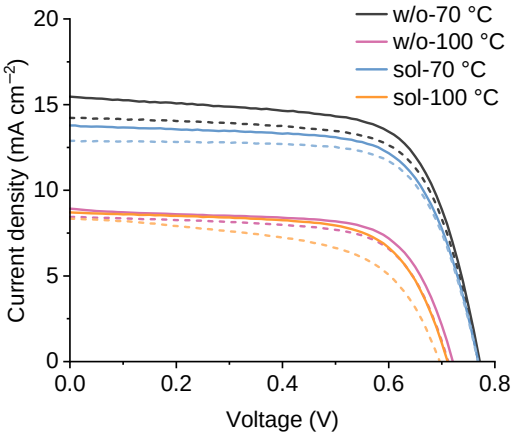

Name	J_{SC} (mA cm^{-2})	V_{OC} (V)	FF	PCE (%)
w/o-70 °C-F	15.46	0.77	0.68	8.08
w/o-70 °C-R	14.23	0.77	0.70	7.61
w/o-100 °C-F	8.92	0.72	0.68	4.39
w/o-100 °C-R	8.44	0.71	0.68	4.06
sol-70 °C-F	13.78	0.77	0.69	7.30
sol-70 °C-R	12.88	0.77	0.71	7.02
sol-100 °C-F	8.71	0.71	0.67	4.15
sol-100 °C-R	8.34	0.70	0.58	3.36

Figure S19. *J–V* curves and performance parameters of the champion devices based on perovskite films post-treated with and without CT mixed solvent, denoted as sol and w/o, respectively, and annealed at different temperatures. All perovskite films are first annealed at 70 °C for 10 min; second 10 min annealing was made at 70 and 100 °C for the cells denoted as 70 °C and 100 °C, respectively. The same condition, **CT-70** °C, was applied for the processing of the ICBA films in the complete cell stacking. In comparison with the w/o-70 °C cells, the slight decrease on the J_{SC} for the sol-70 °C cells might be caused by the residual TCB, as the TCB was likely unable to be completely removed under 70 °C.

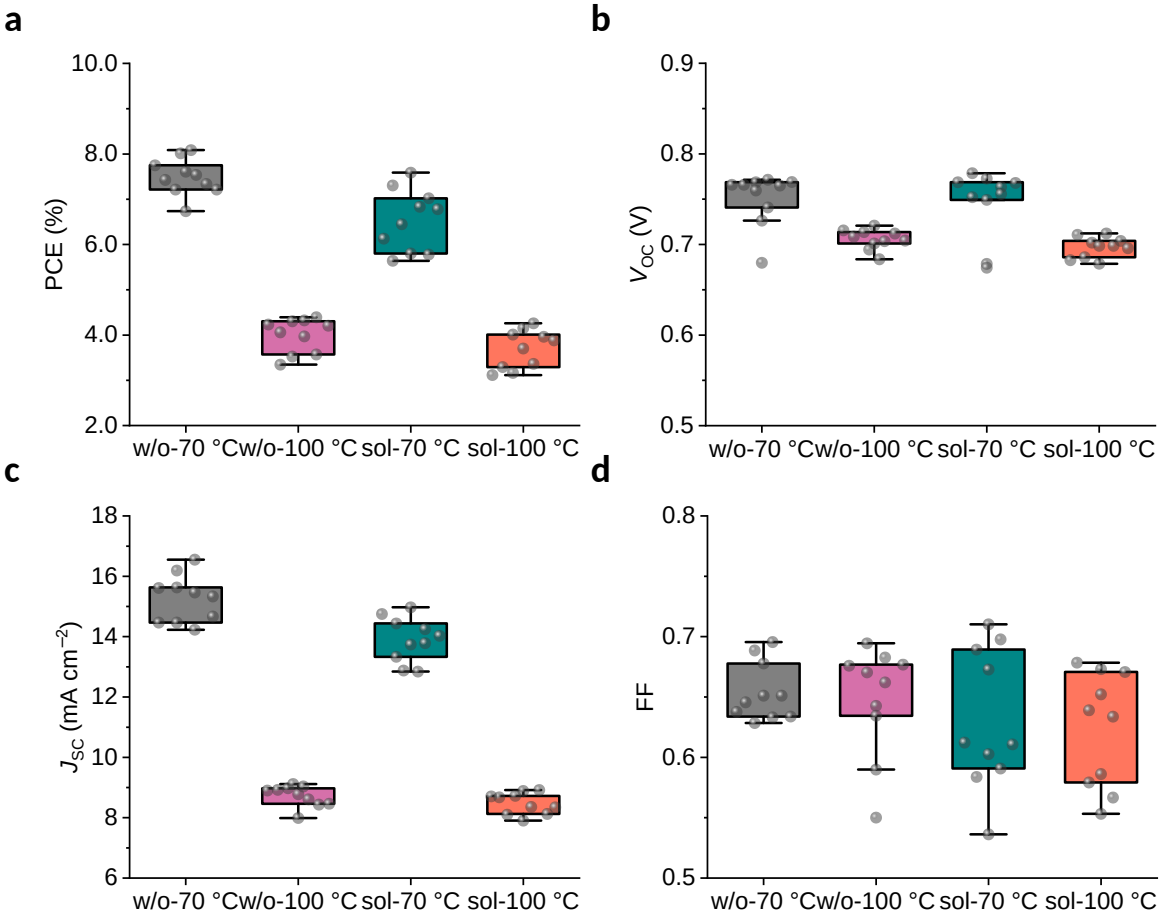

Figure S20. Distributions of (a) PCE, (b) V_{OC}, (c) J_{SC}, and (d) FF values derived from forward and reverse *J*–*V* scans for devices based on perovskites treated with and without CT mixed solvent (denoted as sol and w/o) and annealed at different temperatures with six samples for each condition. The same condition, **CT-70** °C, was applied for the processing of the ICBA films in the complete cell stacking.

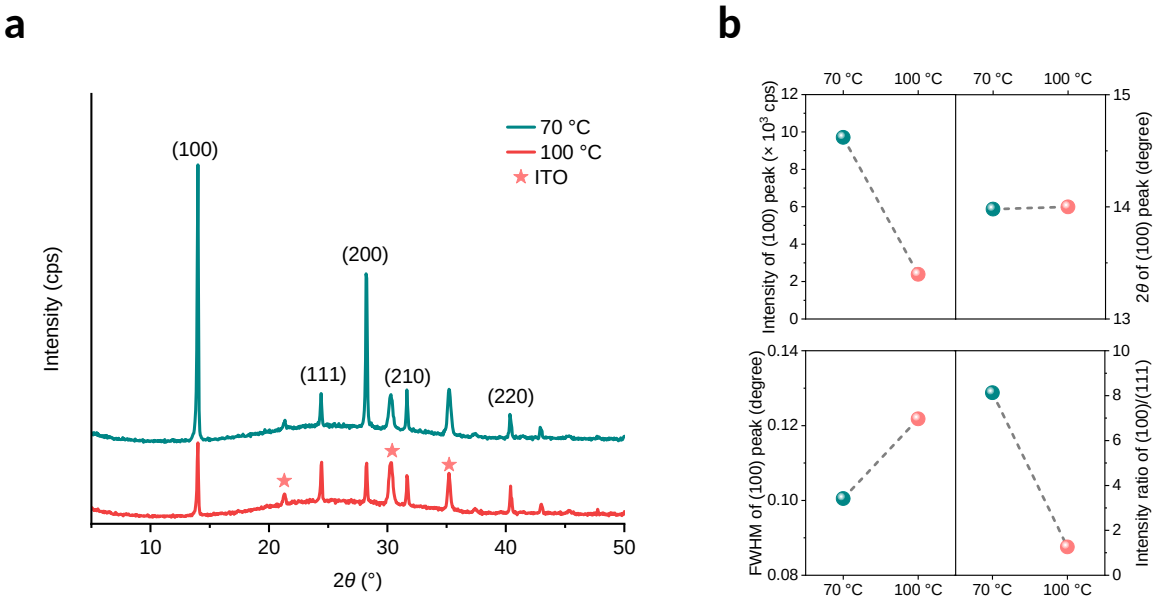

Figure S21. (a) XRD patterns of perovskite films annealed at 70 °C and 100 °C, respectively. (b) Intensity, 2θ values, the full width at half maximum (FWHM) of the (100) peaks, and proportions of the intensity of (100) peak/(111) peak of the perovskite films annealed at 70 °C and 100 °C. A thin layer of PMMA was coated onto the perovskite films to prevent oxidation during the measurement.

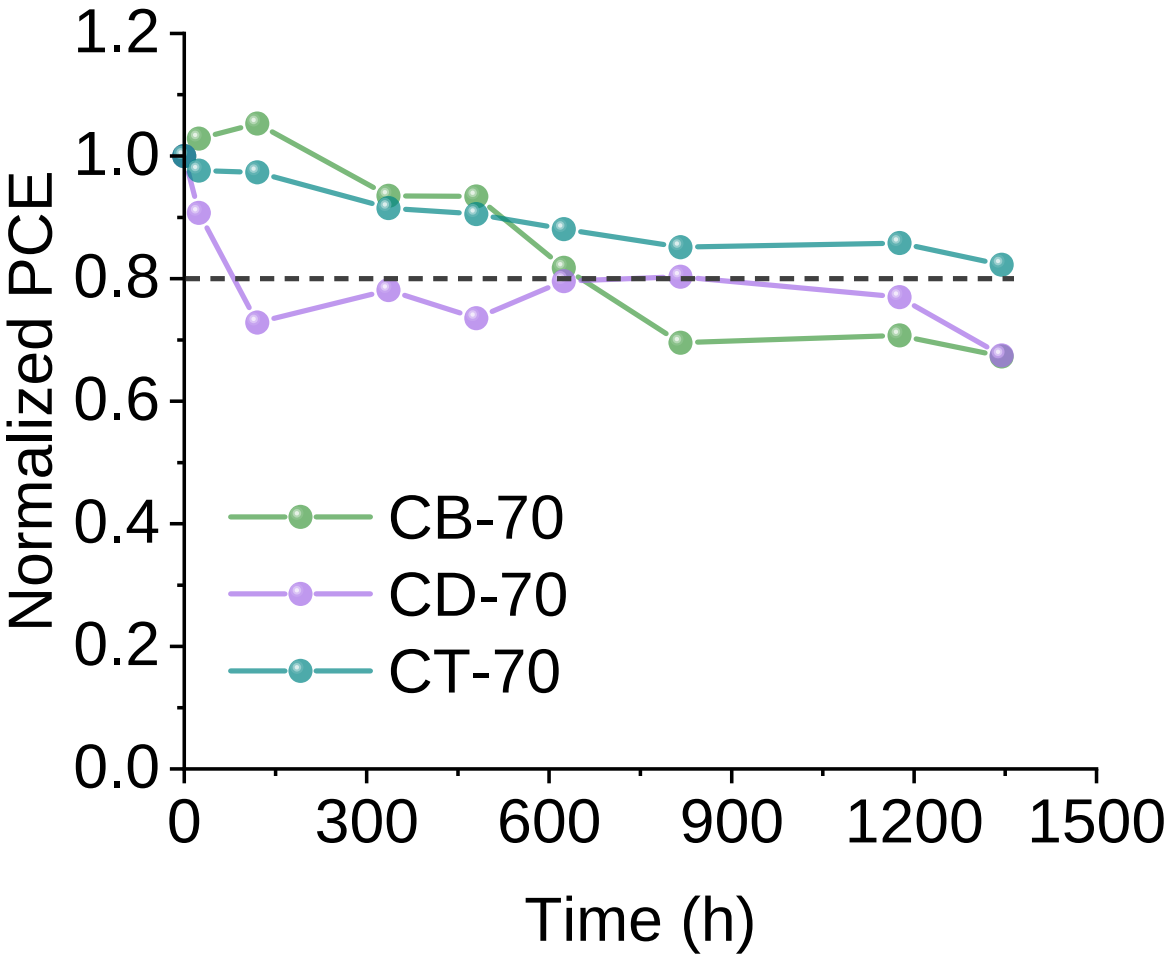

Figure S22. Shelf-stability of unencapsulated cells with ICBA films processed from **CB-70**, **CD-70**, or **CT-70**. For this test, devices were stored in the dark in an N_2-filled glovebox.

Figure S23. Water contact angles of (a) **CB-70**, (b) **CD-70**, and (c) **CT-70** processed ICBA films fabricated on perovskite layer.

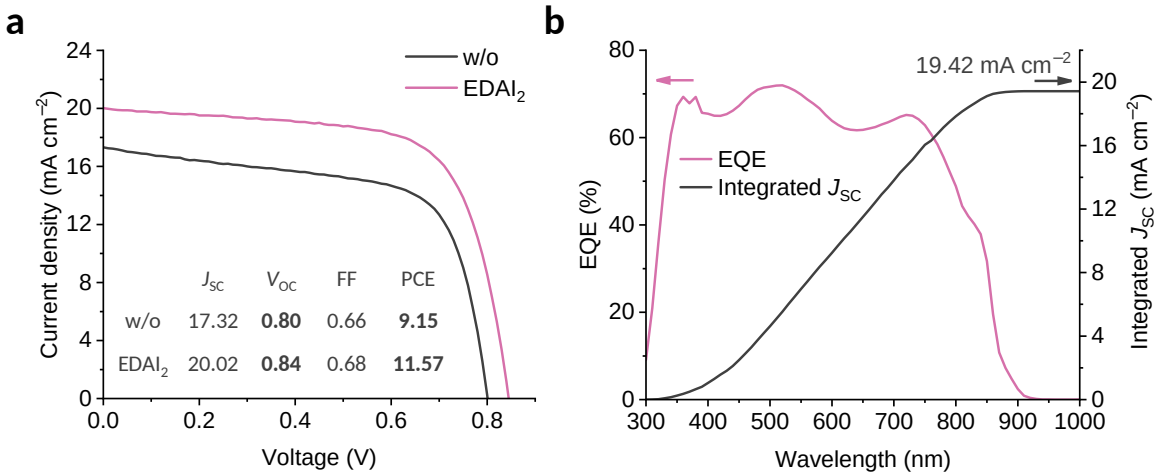

Figure S24. (a). *J*–*V* curves of the solar cells fabricated with and without $EDAI_2$ post-treatment. (b). EQE spectra of the $EDAI_2$-treated devices. The integrated J_{SC} of $EDAI_2$-treated devices is 19.42 mA cm^{-2}. For the post-treatment, 150 µL $EDAI_2$ solution in IPA/toluene (1/1, v/v) was dynamically spin-coated onto perovskite films. The ICBA films were fabricated with the **CT-70** process.

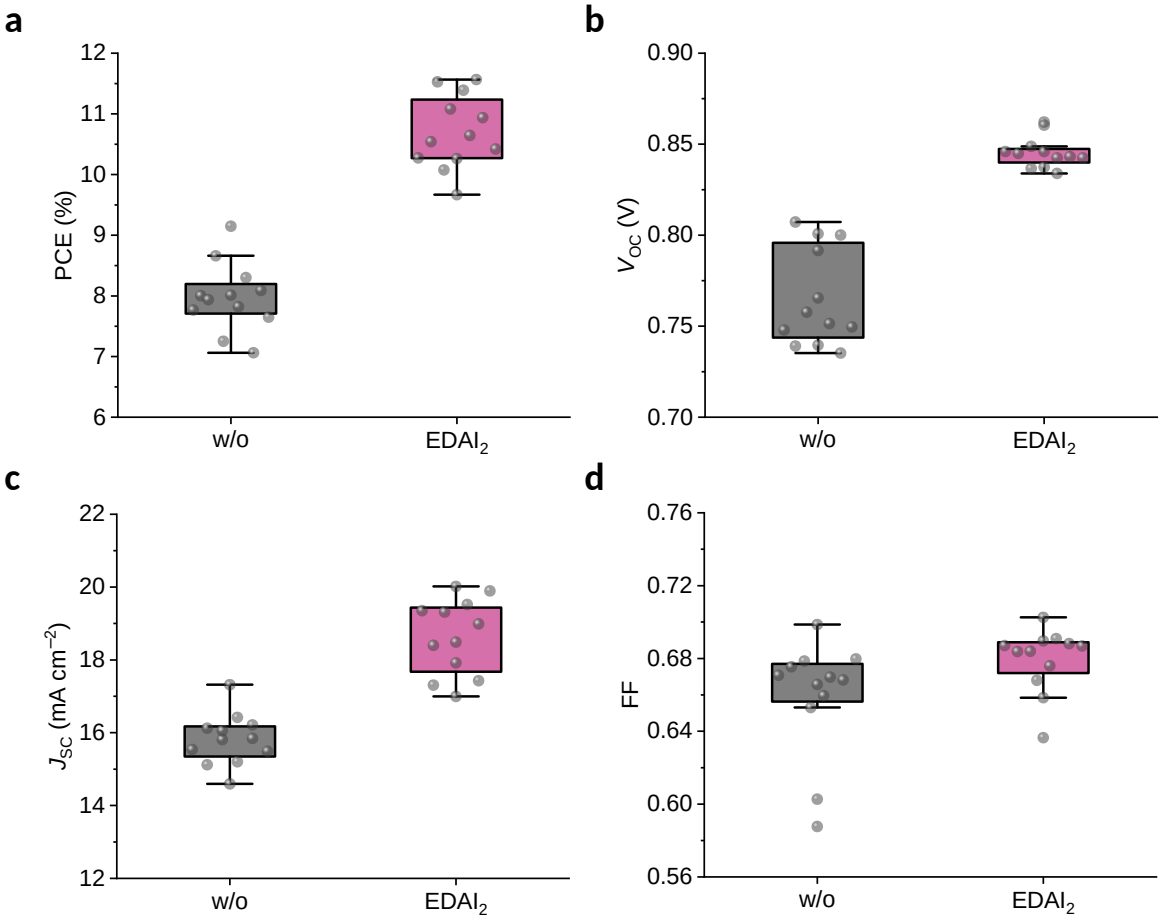

Figure S25. Distributions of (a) PCE, (b) V_{OC}, (c) J_{SC}, and (d) FF values derived from forward and reverse *J*–*V* scans for devices fabricated with and without $EDAI_2$ post-treatment with six samples for each condition. The ICBA films were fabricated with **CT-70** process.

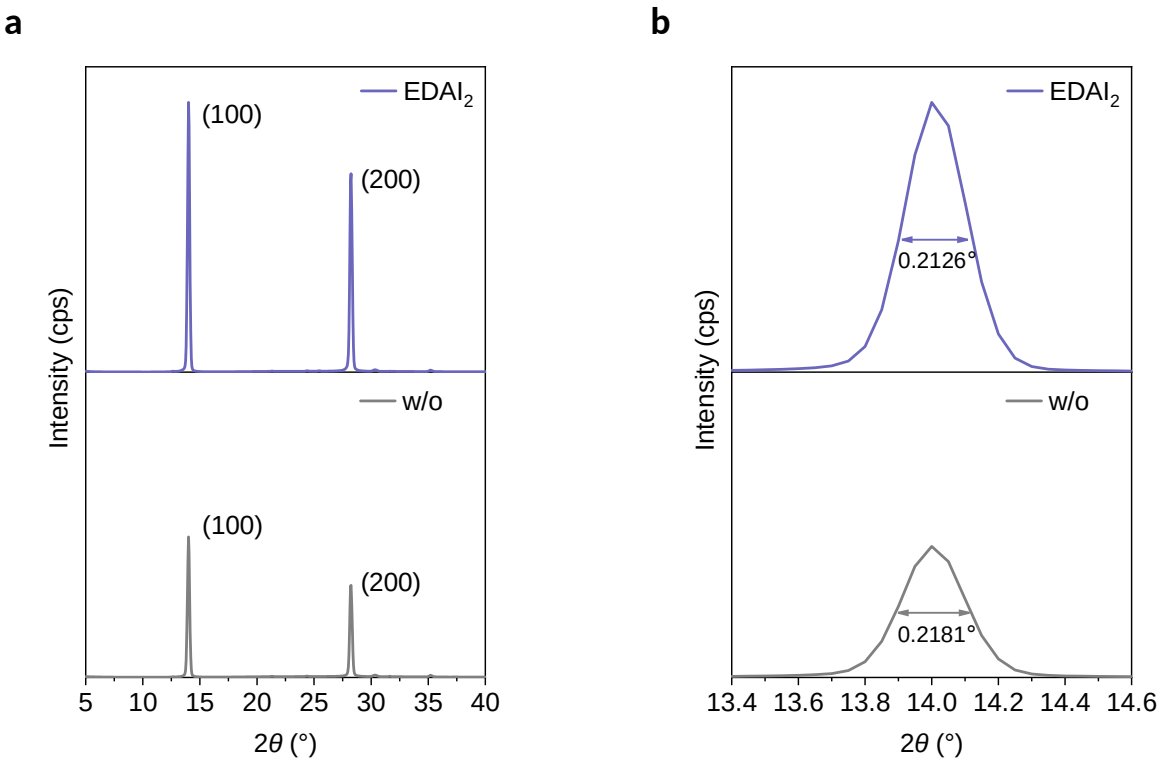

Figure S26. (a) XRD patterns of perovskite films with and without $EDAI_2$ treatment, respectively. (b) The (100) peak of the perovskite films with and without $EDAI_2$ treatment. The ranges of both *x* and *y* axes are kept the same for the stack figures. A thin layer of PMMA was coated onto the perovskite films to prevent oxidation during the measurement.